Biosensors and Bioelectronics 28 (2011) 368–372

Contents lists available at ScienceDirect

Biosensors and Bioelectronics

journal homepage: www.elsevier.com/locate/bios

Electrical impedimetric biosensors for liver function detection

Ya-Hsuan Chuang[a], Yun-Tzu Chang[a], Kuo-Liang Liu[a], Hwan-You Chang[b], Tri-Rung Yew[a,*]

[a] National Tsing Hua University, Department of Materials Science and Engineering, 101, Sec. 2, Kuang-Fu Road, Hsinchu 30013, Taiwan
[b] National Tsing Hua University, Department of Life Science, 101, Sec. 2, Kuang-Fu Road, Hsinchu 30013, Taiwan

ARTICLE INFO

Article history:
Received 8 June 2011
Accepted 19 July 2011
Available online 26 July 2011

Keywords:
Biosensor
Human serum albumin
Electrical impedimetric
3-Aminopropyltriethoxysilane
Lab-on-a-chip

ABSTRACT

In this study, electrical impedimetric biosensors composed of Au-electrodes were fabricated for the quantitative detection of human serum albumin (HSA), an essential biomarker of liver function. The Au-electrodes were fabricated via a single-step photolithography process, and can be easily integrated in biochips for assessing liver function in the future. The glass sensing surface between two adjacent Au-electrodes was modified with 3-aminopropyltriethoxysilane (APTES) to improve the biocompatibility for its subsequent binding to anti-human serum albumin (AHSA). The sensing surface without AHSA binding was blocked using skim milk powders, preventing possible non-specific bonding HSA conjugation. Biosensors were used to measure HSA concentration for liver function detection. The impedance between two adjacent Au-electrodes of the biosensors applied with various HSA concentrations was directly measured, and quantified using an electrochemical impedance spectroscopy system under AC conditions. The results of plotting both values in log scales indicated the impedance increased linearly with HSA conjugation increase. The limit of HSA detection was about $2'10^{-4}$ mg/ml using the electrochemical impedimetric biosensor proposed in this work. This study demonstrates the feasibility of using electrochemical impedimetry as a bio-sensing mechanism to quantify human serum albumin concentration. The sensor proposed in this work also displays great potential for assessing liver function because of its simple detection mechanism, ease of biochip integration, and low cost.

1. Introduction

The human liver has a wide range of functions, including the processing of nutrients, metabolizing of medication, and body detoxification (Khetani and Bhatia, 2008; Rockeyl and Bissell, 2006). Liver function assessment is vital to clinical functions. Enzyme tests from glutamic oxaloacetic transaminase (GOT), glutamic pyruvic transaminase (GPT) (Morimoto et al., 2007; Moser et al., 1997), and human serum albumin (HSA) (Ulrich et al., 2002) are frequently used to indicate liver function. The HSA is synthesized and secreted by liver, and is the most abundant protein in the circulatory system. An HSA biosensor that can detect a wide range of HSA concentrations is vital for assessing liver function. In addition to responding rapidly and possessing high sensitivity, biosensors that assess liver function also need be easily integrated into a lab-on-a-chip (LOC) device, and capable of real-time detection. (Ronkainen et al., 2010; Vadgama and Crump, 1992; Grieshaber et al., 2008; Song et al., 2007)

Various methods to detect HSA using electromechanical, optical, or mechanical systems have been proposed. (Huang et al., 2007; Chuang et al., 2006; Tolani et al., 2009; De et al., 2009; Lin et al., 2004) However, electrochemical systems remain the most common biosensing method (Luong et al., 2008). An HSA detection of 0.1–0.4 mg/ml (Huang et al., 2007), or approximately 10^3 mg/ml (Chuang et al., 2006), can be achieved using an amperometric biosensor and cyclic voltammetry measurement. An alternative approach to increase HSA detection sensitivity is the use of polymer nanowires to sense current–voltage measurements (Tolani et al., 2009), increasing sensitivity to 3×10^{-3} mg/ml. However, this approach has several drawbacks, including the time-consuming preparation process, relatively high cost, and additional operation procedures.

Therefore, a detection method that simplifies the albumin sensing procedures is critical. Additionally, a specific antibody and antigen conjugation that can increase selectivity and sensitivity, as well as HSA concentrations, must be developed. This study proposes HSA detection by calibrating the electrical contribution of HSA at various concentrations using a test pattern comprised of Au-electrodes and modified with antibodies. The biosensors are fabricated using single-step photolithography, and can be easily and directly integrated into biochips. This study discusses the feasibility of using this approach in future specific and quantitative HSA sensing applications.

* Corresponding author. Tel.: +886 936347230; fax: +886 3 5722366.
E-mail address: tryew@mx.nthu.edu.tw (T.-R. Yew).

0956-5663/$ – see front matter © 2011 Elsevier B.V. All rights reserved.
doi:10.1016/j.bios.2011.07.049

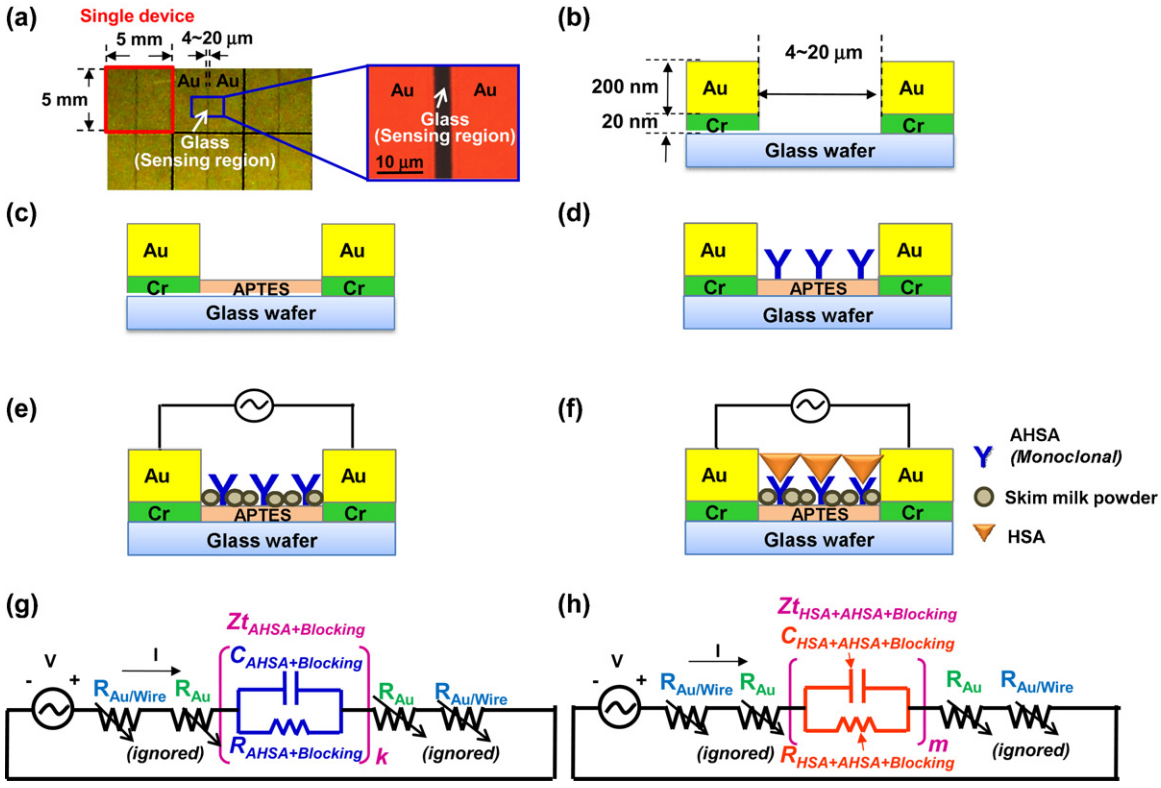

Fig. 1. (a) The optical microscopy of Au-electrodes array with a red boxed area indicating a 5 mm × 5 mm single device cut for HSA sensing. The detailed process flow schematics including (b) cross-section of the patterned 20 nm Cr/200 nm Au layer on glass, selective (c) APTES vapor deposition on glass, (d) AHSA immobilization on APTES, (e) skim milk powder blocking, and (f) HSA conjugation. The equivalent circuit models of (g) pre- and (h) post-HSA conjugation with *k* and *m* units of double-layer capacitance and resistance, respectively.

2. Materials and methods

2.1. Fabrication of Au-electrodes

The Au-electrode arrays of glass-based biosensors were fabricated using single-step photolithography. First, the photoresist was spin-coated and patterned onto a glass substrate before sequentially depositing a 20 nm adhesion layer of chromium (Cr) and a 200 nm layer of gold (Au) using an electron beam evaporator. The lift-off process using ultrasonic methods completed the fabrication of Au-electrode array test patterns. The spacing (L) between two adjacent Au-electrodes for HSA sensing ranged from 4 μm to 20 μm, and the width (W) of the electrode was approximately 5 mm. The optical microscopy image of the Au-electrode array is displayed in Fig. 1a, and the Au-electrode schematic in Fig. 1b. The single device with a size of 5 mm × 5 mm, as shown in red boxed area in Fig. 1a, was cut from the array before sensing. A large amount of the single device could be fabricated on a glass substrate using the abovementioned Au-electrode array fabrication process.

2.2. Antibody immobilization

The Au-electrode test patterns were cleaned using isopropyl alcohol (IPA) for 15 min and a piranha solution (1:3 H_2O_2-concentrated H_2SO_4) for 30 min, rinsed with deionized (DI)-water, and dried using a N_2 flow (Lu et al., 2008). During this process, the glass surface was functionalized with hydroxyl groups. Amine groups were attached to the surface via a 3-aminopropyltriethoxysilane (APTES) vapor reaction, as displayed in Fig. 1c. This reaction was carried out by placing the pretreated patterns and a small dish containing 40 μl of APTES in a desicator for 30 min before washing and drying the test patterns to remove residual chemicals. The silanized APTES surface was incubated in 0.1 M phosphate buffered saline (PBS) containing 1 μg/ml of anti-human serum albumin (AHSA) at 37 °C and pH 7, and continuously agitated as demonstrated in Fig. 1d. The covalent binding of self-assembled APTES on the hydroxyl-terminated silicon oxide substrates (Robert et al., 2008) immobilized AHSA on the sensing region for HSA detection. The AHSA-modified test patterns were treated with 5% skim milk powders for 1 h (Mailti et al., 1993) to block untreated and non-specific sites. The test pattern was then dried by using N_2 for electrochemical measurement to obtain background impedance, as shown in Fig. 1e, before HSA detection. Background impedance (at a value of 1×10^8–2×10^8 Ω in this case) must be sheltered from moisture effects and poor-contact issues, which can vary background levels and degrade detection accuracy.

2.3. Human serum albumin conjugation

HSA sensing, the AHSA-modified sensor was immersed in PBS solution with HSA concentrations ranging from 6 mg/ml to 2×10^{-12} mg/ml at room temperature for 1 h, and under constant agitation. Thereafter, the test patterns conjugated with HSA were thoroughly rinsed using DI-water to remove unbound antigens, and dried using N_2 flow prior to electrochemical measurement, as shown in Fig. 1f.

2.4. Electrical impedimetric measurement

The impedance between two adjacent Au-electrodes applied with various concentrations of HSA was measured and quantified using an electrochemical impedance spectroscopy system under AC conditions in a dry environment. The impedance was measured using a Hewlett Packard 4284A Precision LCR meter with a sinu-

soidal AC voltage of 10 mV (peak-to-peak voltage) in amplitude at the frequency range of 20 Hz–100 kHz was applied for measurements.

The proposed equivalent circuit for each single device of the AHSA-modified electrochemical biosensor is displayed in Fig. 1g. The $R_{Au/wire}$ is the contact resistance between the Cu wire and the Au-electrode, and R_{Au} is the resistance of the Au-electrode. The parallel components of $C_{AHSA+Blocking}$ and $R_{AHSA+Blocking}$ are the unit double-layer capacitance and unit resistance respectively, which are contributed by each unit of AHSA/blocking-agent/APTES (i.e., one AHSA with adjacent blocking-agent and underneath APTES). To calculate the total background impedance ($Zt_{AHSA+Blocking}$), the contribution from $R_{Au/wire}$ and R_{Au} shown in Fig. 1g can be ignored due to their insignificant values. The total background impedance ($Zt_{AHSA+Blocking}$) was contributed primarily from all AHSA/blocking-agent/APTES units (assuming k units in the case) on the glass area between two Au-electrodes. In this work, the process was optimized for uniform and saturated AHSA modification so as to keep the total background impedance ($Zt_{AHSA+Blocking}$) of each single device at a constant value ($\sim 10^8\ \Omega$) before its use for HSA detection (i.e., nearly constant k value).

The proposed equivalent circuit of the biosensors after HSA conjugation is shown in Fig. 1h, including $R_{Au/wire}$, R_{Au}, and total impedance ($Zt_{HSA+AHSA+Blocking}$). Similarly, the contributions from $R_{Au/wire}$ and R_{Au} can be ignored. The parallel components of $C_{HSA+AHSA+Blocking}$ and $R_{HSA+AHSA+Blocking}$ are the unit double-layer capacitance and unit resistance, respectively, which are contributed by each unit of HSA/AHSA/blocking-agent/APTES (i.e., one HSA with adjacent AHSA, blocking-agent, and underneath APTES). The total background impedance ($Zt_{HSA+AHSA+Blocking}$) was contributed primarily from all the HSA/AHSA/blocking-agent/APTES units (m units assuming m number of HSA molecules in the case) on the glass area between two Au-electrodes. The value of m is proportional to HSA concentration.

Based on above, the HSA concentration could be detected by quantifying the relationship between the changes of total impedance (ΔZt_{Diff}) versus the HSA concentrations. This can be carried out by measuring the impedance pre- and post-HSA conjugation at various HSA concentrations and the impedance change (ΔZt_{Diff}) can be calculated using the equation: $\Delta Zt_{Diff} = Zt_{HSA+AHSA+Blocking} - Zt_{AHSA+Blocking}$.

3. Results and discussion

3.1. Verification of surface modification and antibody immobilization

For specific HSA detection, the sensing surface was functionalized with an AHSA protocol and optimized, as described in the methods section. Ensuring the presence of AHSA on the biosensor surface is vital before HSA sensing. This can be determined by applying the fluorescent dye labeled anti-IgG antibody to the sensing surface with AHSA functionalization and skim milk powder for blocking. Fig. 2a indicates an absence of green fluorescence on the APTES-modified glass (APTES/glass) surface with AHSA functionalization and skim milk powder blocking under a fluorescence microscope prior to the application of the fluorescent dye labeled anti-IgG antibody. Conversely, Fig. 2b shows that the surface of AHSA-functionalized APTES/glass glows green after applying the fluorescent dye labeled anti-IgG antibody. It indicates the APTES/glass area of the test patterns was successfully functionalized with AHSA. This also suggests the AHSA conjugated on the APTES/glass retained its biological activity (Tolani et al., 2009).

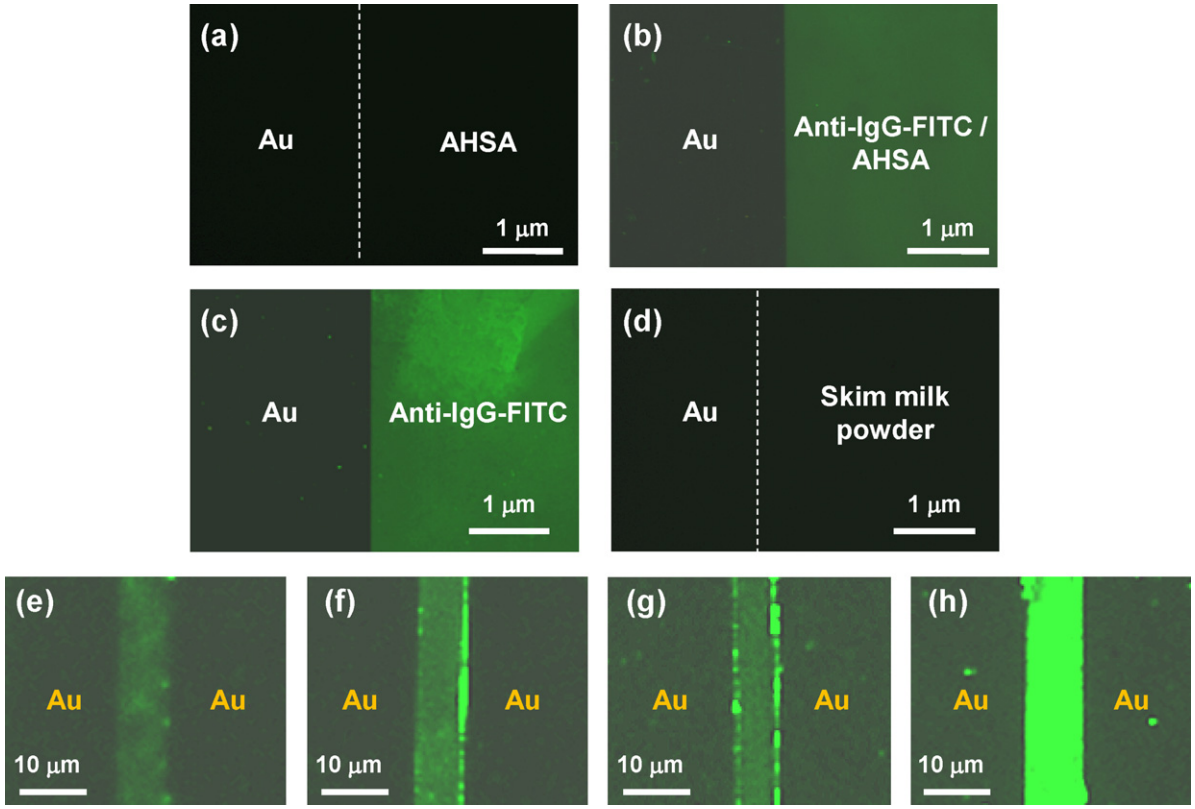

Fig. 2. Fluorescence microscopy images of the biosensors. (a) Pre- and (b) post-fluorescent dye* labeled anti-IgG antibody on APTES modified test pattern with AHSA functionalization and skim milk powder blocking. After applying the fluorescent dye labeled anti-IgG antibody on the test pattern (c) without- and (d) with-skim milk powder treatment on APTES/glass surface. The biosensors with different concentrations of HSA, (e) 2×10^{-8} mg/ml, (f) 2×10^{-6} mg/ml, (g) 2×10^{-3} mg/ml, (h) and 2×10^{-1} mg/ml, and conjugated with fluorescent dye labeled HSA antibody (*Polyclonal*). *Fluorescent dye: FITC.

Furthermore, the blocking effect of skim milk powder was confirmed via fluorescence microscopy. Fig. 2c shows that the fluorescent dye labeled anti-IgG antibody bound directly to the APTES/glass surface without the skim milk powder blocking. However, the APTES/glass surface treated with skim milk shows no fluorescence in Fig. 2d following immobilization of fluorescent dye labeled anti-IgG antibody. Fig. 2c and d suggest skim milk powders could block the untreated and non-specific sites effectively.

3.2. Verification of various concentrations of HSA immobilization

Upon confirmation of the blocking effect and functionalization of AHSA, it was necessary to ensure the conjugation of HSA increased in correlation with the HSA concentration. Fig. 2e–h shows the fluorescent images of the AHSA/APTES/glass upon bonding with a fluorescent dye labeled HSA antibody (*Polyclonal*), and after the addition of HSA in concentrations of 2×10^{-8} mg/ml, 2×10^{-6} mg/ml, 2×10^{-3} mg/ml, and 2×10^{-1} mg/ml, respectively. The brightness of the fluorescent image increased in correlation with the applied HSA concentrations, which indicates that HSA can be immobilized on the sensing region and used for electrical measurements.

3.3. Equivalent circuit model

To characterize the electrochemical albumin-sensing module following HSA conjugation on the biosensors, Fig. 3a shows the phase angle with a measuring frequency of 20 Hz–100 kHz. In Fig. 3a, three data points were excluded as a data disparity was caused by unstable equipment during the initial measurements taken at low frequencies. At low frequencies, the phase angle was lower than −90°. Additionally, the current contribution from 0.2 mg/ml HSA under DC conditions is approximately $7 \times 10^{-13} \pm 1.4 \times 10^{-14}$ A at 1 V applied, and the resistance contributed by HSA/AHSA/blocking-agent/APTES unit ($R_{HSA+AHSA+Blocking}$) is approximately 10^{13} Ω. Therefore, HSA/AHSA/blocking-agent/APTES can be regarded as a high-impedance material at DC. The phase angle increased at higher frequencies (>50 kHz) and reached −85° at 100 kHz, indicating unit double-layer capacitance ($C_{HSA+AHSA+Blocking}$) contributed significantly to the impedance which is similar to the capacitive conduction reported. (Berggren et al., 2000) Therefore, the contribution of resistance component ($R_{HSA+AHSA+Blocking}$) could be ignored. Based on above, a measuring frequency of 100 kHz was applied to maintain a capacitance domination of the impedance signal.

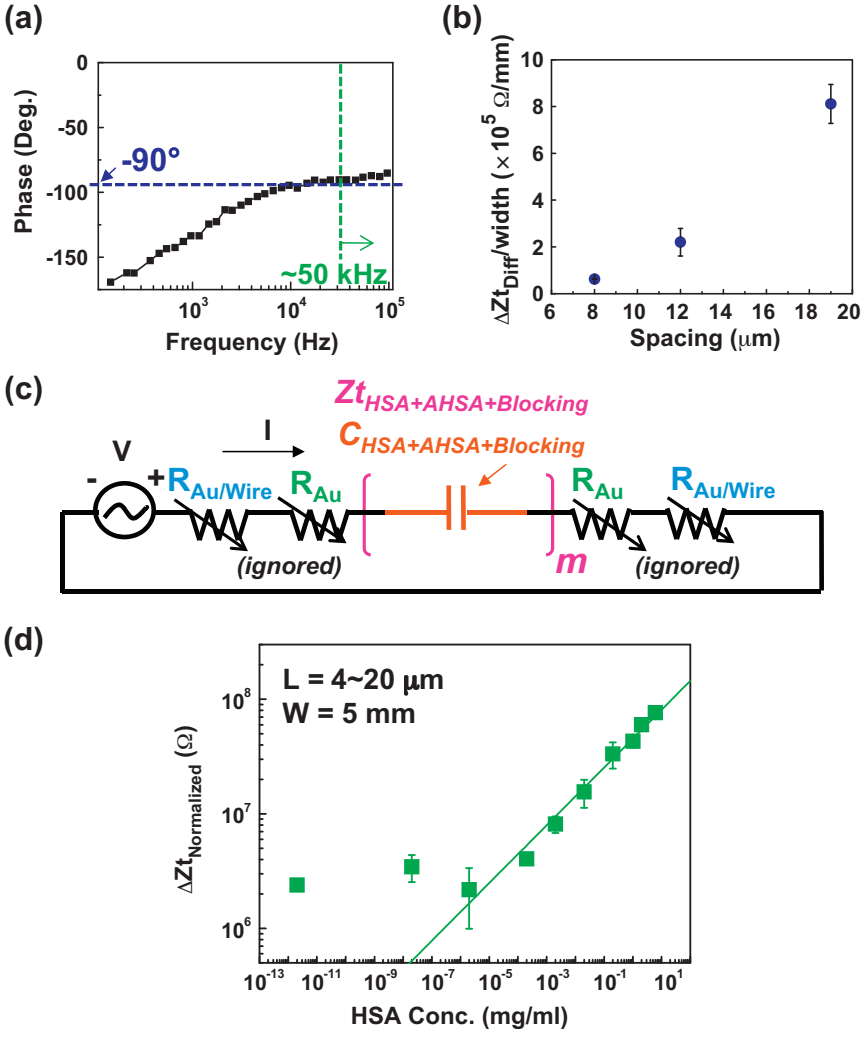

Fig. 3. (a) Phase and frequency plot. (b) Impedance variation per unit width of gold electrodes versus different spacing between two adjacent Au-electrodes. (c) The simplified equivalent circuit of the biosensor with m units of capacitance (contributed by one HSA and adjacent AHSA, blocking agent, and APTES for each unit) connected in series after HSA conjugation, as explained in section 3.3. (d) The impedance change after HSA-immobilized ($\Delta Zt_{Normallized} = \Delta Zt_{Diff} \times W/L$) measured at 100 kHz versus different HSA concentrations. $\Delta Zt_{Diff} = Zt_{HSA+AHSA+Blocking} - Zt_{AHSA+Blocking}$, W as Au-electrode width (5 mm), and L as the spacing (4–20 μm) between two Au-electrodes.

For impedance measurements, 0.2 mg/ml of HSA was applied to biosensors dispersed between the Au-electrodes. Fig. 3b displays the impedance change per unit-width of Au-electrodes (ΔZt_{Diff}/width), by dividing the total impedance change ΔZt_{Diff} with Au-electrode width (W = 5 mm), between two Au-electrodes with a spacing (L) of 8, 12, and 19 μm. Though the resistance increased with the increase of Au-electrode spacing, the amplification was not linear. It is suspected that the HSA conjugation on the varied sensing area was not as uniform as expected.

Using the preceding phase angle analysis in Fig. 3a and the relationship between ΔZt_{Diff}/width and electrode spacing in Fig. 3b, the equivalent circuit model of the biosensors with HSA conjugation displayed in Fig. 1h can be further simplified. Since the double-layer capacitance at 100 kHz dominates electrical conduction, the resistance component connected in parallel can be ignored. Consequently, the equivalent circuit of the biosensor with HSA conjugation can be simplified as that in Fig. 3c, with the conduction similar to the capacitive biosensors reported. (Berggren et al., 2000) Assuming the unit double-layer capacitors are connected in series between two electrodes, the total capacitance per unit width ($Ct_{HSA+AHSA+Blocking}$/width) can be obtained by dividing the unit double-layer capacitance with the numbers of capacitors connected, i.e. $Ct_{HSA+AHSA-Blocking}$/width = $(1/m)C_{HSA+AHSA+Blocking}$/width. The increase of HSA concentration (i.e. larger value of m) will lead to the decrease of $Ct_{HSA+ASHA+Blocking}$/width and the increase of total impedance per unit-width ($Zt_{HSA+AHSA+Blocking}$/width) as $Zt_{HSA+AHSA+Blocking}$/width = $(1/j\omega Ct_{HSA+AHSA+Blocking})$/width = $(m/j\omega C_{HSA+AHSA+Blocking})$/width. Besides, as the total background impedance ($Zt_{AHSA+Blocking}$) is kept at a constant value pre-HSA conjugation in this work, the total impedance change per unit width (ΔZt_{Diff}/width) between pre- and post-HSA conjugation will increase with the increase of HSA concentration.

3.4. Impedance contribution of various HSA concentrations

The impedance contribution from various HSA concentrations at a fixed frequency (F = 100 kHz) can be determined via the impedance change following HSA conjugation. The HSA concentration value can be obtained by correlating the normalized total impedance change ($\Delta Zt_{Normallized} = \Delta Zt_{Diff} \times W/L$, W as the Au-electrode width and L as the spacing between two adjacent Au-electrodes) with the HSA concentration (HSA conc.). In Fig. 3d, the data were summarized from the HSA sensing using the devices with L = 4–20 μm and W = 5 mm. Fig. 3d indicates that the impedance change increases linearly with the increase of HSA concentration (both plotted in log scales). According to equivalent circuit models, the increase of impedance indicates more HSA conjugation between the two adjacent Au-electrodes. Therefore, the HSA concentrations in the sample can be determined via the measured impedance change, according to the relationship shown in Fig. 3d. It shows that the limit of HSA detection is about 2×10^{-4} mg/ml, using the proposed electrochemical impedimetric biosensor.

For the nonlinear part in Fig. 3d with HSA concentrations lower than 2×10^{-4} mg/ml, the normalized impedance is sustained at approximately 3×10^6 Ω for the biosensors. This suggests that HSA conjugation is discontinuous between two adjacent Au-electrodes. According to theoretical calculations, the size of HSA molecule is approximately 8 nm × 8 nm × 3 nm. For the smallest spacing (L = 4 μm, W = 5 mm), a minimum number of 10^8–10^9 HSA proteins ($m \cong 10^8$–10^9) are required for sequential arrangement, to establish a continuous connection between two adjacent Au-electrodes. In this study, the limit of detection of 2×10^{-4} mg/ml indicates that at least 10^{12} numbers of individual classes of proteins ($m \cong 10^{12}$) per milliliter were connected. As the HSA concentration is lowered to 2×10^{-6} mg/ml, it indicates an approximate number of 10^{10} HSA ($m \cong 10^{10}$) per milliliter of solution, which is close to the theoretical value of 10^8–10^9. Therefore, it is likely a discontinuous HSA conjugation between two adjacent Au-electrodes at such a low concentration.

4. Conclusion

This study presents an albumin-sensing system comprising Au-electrode arrays, which utilizes an electrical impedimetric sensing mechanism for liver function detection. The fluorescent image tests verified that the AHSA maintained biological activity post-immobilization, as demonstrated by the selective functionalization of HSA on AHSA-modified glass. In this electrical impedimetric characterization, the HSA/AHSA/blocking-agent/APTES units were connected and the charge transfer is via capacitor coupling at 100 kHz. The concentration of the HSA conjugated between adjacent gold electrodes can be directly measured and quantified by the impedance change of biosensors pre- and post-HSA conjugation. The limit of detection is about $\sim 2 \times 10^{-4}$ mg/ml for the proposed albumin sensor.

In addition to the single-step photolithography fabrication, the simple detection mechanism provides the Au-electrode biosensors with easy fabrication and low-cost advantages as many devices can be fabricated on the glass simultaneously. Therefore, it exhibits great potential for the future application in liver function detection. The high-sensitivity innovative biosensor can be integrated into the biochip directly and with ease. The results reveal the potential benefits on wide range analytical applications in medical, biological, biotechnological, and environmental fields.

Acknowledgments

We thank NSC (grants: NSC98-2120-M-007-003) for financial support. We also thank NCTU-NFC and NTHU-TCSFT for facility support, and the valuable suggestions from Prof. Chen-Hsien Liu, Prof. Hwan-You Chang, Prof. Chi-Young Lee, and Shiang-Jie Yen at NTHU, Prof. Hwei-Ling Peng and Prof. Long Hsu at NCTU, and Shau-Feng Chang at ITRI.

References

Berggren, C., Bjarnason, B., Johansson, G., 2000. Electroanalysis 13, 173–180.
Chuang, M.C., Liu, C.C., Yang, M.C., 2006. Sens. Actuators B 114, 357–363.
Grieshaber, D., MacKenzie1, R., Vörös1, J., Reimhult, E., 2008. Sensors 8, 1400–1458.
Huang, C.J., Lu, C.C., Lin, T.Y, Chou, T.C., Lee, G.B., 2007. J. Micromech. Microeng. 17, 835–842.
Khetani, S.R., Bhatia, S.N., 2008. Nat. Biotechnol. 26 (1), 120–126.
Lin, T.Y., Hu, C.H., Chou, T.C., 2004. Biosens. Bioelectron. 20, 75–81.
Lu, Y.C., Chuang, Y.S., Chen, Y.Y., Shu, A.C., Hsu, H.Y., Chang, H.Y., Yew, T.R., 2008. Biosens. Bioelectron. 23, 1856–1861.
Luong, J.H.T., Male, K.B., Glennon, J., 2008. Biotechnol. Adv. 26, 492–500.
Maiti, N.K., Saini, S.S., Singh, R., Oberoi, M.S., Sharma, S.N., 1993. Comp. Immunol. Microb. 16 (3), 245–250.
Moser, I., Jobst, G., Svasek, P., Varahram, M., Urban, G., 1997. Sens. Actuators B 44, 377–380.
Morimoto, K., Upadhyay, S., Higashiyama, T., Ohgami, N., Kusakabe, H., Fukuda, K., Suzuki, H., 2007. Sens. Actuators B 124, 477–485.
De, M., Rana, S., Akpinar, H., Miranda, O.R., Arvizo, R.R., Bunz, U.H.F., Rotello, V.M., 2009. Nat. Chem. 1, 461–465.
Robert, M.P., Sandrine, R.A., Yves, J.C., 2008. Langmuir 24, 12963–12971.
Rockeyl, D.C., Bissell, D.M., 2006. Hepatology 43 (2), S113–S120.
Ronkainen, N.J., Halsall, H.B., Heineman, W.R., 2010. Chem. Soc. Rev. 39, 1747–1763.
Song, M.J., Yun, D.H., Min, N.K., Hong, S.I., 2007. J. Biosci. Bioeng. 103 (1), 32–37.
Tolani, S.B., Craig, M., DeLong, R.K., Ghosh, K., Wanekaya, A.K., 2009. Anal. Bioanal. Chem. 393, 1225–1231.
Ulrich, K.H., Chuang, V.T.G., Otagiri, M., 2002. Biol. Pharm. Bull. 25 (6), 695–704.
Vadgama, P., Crump, P.W., 1992. Analyst 117, 1657–1670.